Using three-dimensional fluorescence excitation–emission matrix spectroscopy with regional integration analysis to determine properties of extracellular polymeric substances in nitrifying sludge at different C/N ratios

Cuizhong Chen[a], Hongwei Sun[b], Junfeng Li[a],*, Hongguang Liu[a], Shengbao Liu[a], Keqing Du[a], Qiugang Wang[a], Yucheng Ren[a], Zhen Wei[a]

[a]*School of Water Conservancy and Architectural Engineering, Shihezi University, Shihezi 8320000, China, Tel. +86-993-2055060; emails: ljfshz@126.com (J. Li), 523528644@qq.com (C. Chen), 123868194@qq.com (H. Liu), 41061806@qq.com (S. Liu), 387861793@qq.com (K. Du), 782823974@qq.com (Q. Wang), 1174823905@qq.com (Y. Ren), 353314511@qq.com (Z. Wei)*
[b]*School of Environmental and Material Engineering, Yantai University, Yantai 264005, China, Tel. +86-156-6690-5528; email: 12821306@qq.com*

ABSTRACT

The influences of the carbon/nitrogen ratio (C/N) on extracellular polymeric substances (EPS) of activated sludge were investigated in four laboratory-scale sequencing batch reactors using three-dimensional excitation–emission matrix (3D-EEM) with fluorescence regional integration (FRI). When the C/N ratio increased from 0 to 15, the polysaccharide (PS), protein (PN), and nuclei acid (NA) contents of tightly bound EPS (TB-EPS) increased, the PS, PN, and NA contents in LB-EPS at the C/N ratio of 0 obviously higher than the C/N ratio of 5, 10, and 15. According to FRI, the C/N ratio had a significant impact on Regions III, IV, and V of EPS, Region V (34%~63%) was the dominant fraction in both types of EPS fractions and TB-EPS and LB-EPS contained similar functional groups, furthermore, the percent fluorescence response ($P_{i,n}$) of humic acid in TB-EPS was dramatically lower than LB-EPS. Meanwhile, a significant decrease of soluble microbial by-product of EPS after nitrification was obtained.

Keywords: Activated sludge; C/N ratio; Extracellular polymeric substance; Three-dimensional excitation–emission matrix; Fluorescence regional integration

1. Introduction

The activated sludge process is one of the major biological wastewater treatment techniques. An undisputed fact that extracellular polymeric substances (EPS) of activated sludge flocs play an important role in the performance of wastewater treatment, and EPS commonly occur in both the interior and on the surface of sludge, originate from metabolism or lysis of microorganisms and the wastewater itself. EPS are important constituents of activated sludge and are composed of loosely bound EPS (LB-EPS) and tightly bound EPS (TB-EPS) [1,2], and have been reported

that the main components of EPS are polysaccharides (PS), proteins (PN), the lesser amounts of humic acid and nuclei acid (NA) [1–4]. Of these, PS were mainly observed in EPS produced from pure cultures, whereas PN were found in higher quantities in the EPS of sludge at many wastewater treatment plants [5]. The character and content of EPS are susceptible to the operational and environmental conditions [6,7]. If certain culture conditions of pH, temperature and carbon and nitrogen sources are induced, then the structure and key component of two kinds of EPS get altered accordingly, LB-EPS and TB-EPS may express different characterizations when the reactors changed the

* Corresponding author.

operational and environmental conditions, resulting in increased or decreased content of the total amount of EPS. Nutritional parameters, such as C/N ratio, affect the microbial physiology, thus impact the character and content of EPS of the sludge.

Many previous studies have shown that the C/N ratio has an important impact on the LB-EPS content and the PS and PN contents in LB-EPS. For example, Ye et al. [8] found that the C/N ratio had no effect on EPS and TB-EPS, but had a significant impact on LB-EPS and its PN and PS components. Furthermore, Wang et al. [9] found that the LB-EPS content changed dramatically when the C/N ratio was increased from 6 to 20. However, other studies have found that the C/N ratio has an important influence on the TB-EPS content. For example, when the C/N ratio was increased from 3.4 to 13.6, a gradual increase in the TB-EPS content was observed [10].

As the EPS may affect the physicochemical properties, structural integrity of microbial aggregates and the biodegradability of sludge, it is very essential to further explore compositional and structural characteristics of EPS. A combination of three-dimensional excitation–emission matrix (3D-EEM) spectra and fluorescence regional integration (FRI) is useful for characterizing organic matter (including EPS) in wastewater [3,11,12]. 3D-EEM fluorescence spectra have been used to test the fluorescent features of organic compounds such as protein, humic, and fulvic acids [13–15], and 3D-EEM spectra have shown the distribution of biodegradable and non-biodegradable materials within EPS [16,17]. Guo et al. [17] assessed sludge hydrolysis using 3D-EEM coupled with FRI to evaluate the compositional characteristics of EPS and dissolved organic matter in disintegrating waste sludge, and the use of FRI in the study by Wei et al. [18] further suggested that Region IV (Table 1) was the main fraction in both types of EPS fractions in two column-type sequencing batch reactors with alternative anoxic/aerobic phases. Sun et al. [19] also utilized 3D-EEM to evaluate the biodegradable and non-biodegradable components of EPS in waste sludge at different heat pretreatment temperatures.

Although many researchers have studied the effects of C/N ratio on EPS properties of activated sludge, their studies were fairly short term and lacked the characterization of influent and effluent EPS by a 3D-EEM technique, and could not investigate the steady change of EPS under certain culture condition for a long period and give spectral information regarding the chemical compositions of EPS

by using 3D-EEM. The aims of this study (running 281 d) were to characterize the chemical compositions (LB-EPS, TB-EPS, polysaccharides, proteins, and nucleic acid contents in EPS) in activated sludge flocs from laboratory-scale sequencing batch reactors (SBRs) under different C/N ratio (0, 5, 10, and 15), and assess the structural variations of influent and effluent EPS in nitrifying sludge using 3D-EEM coupled with FRI.

2. Materials and methods

2.1. Activated sludge systems

Four SBRs were applied with inner and outer diameters of 14 and 15 cm, respectively, and effective volumes of 5 L. A temperature control system was used to maintain a constant temperature of 25°C ± 1°C within each reactor. Each reactor had three sidewall ports in which sensors were inserted to monitor dissolved oxygen (DO), pH, and the oxidation–reduction potential. The synthetic wastewater employed was composed of NH_4Cl, KH_2PO_4, C_2H_5OH, and microelements [20]. Inoculated sludge was obtained from an aeration basin at Lanzhou Municipal Wastewater Plant in Gansu Province, China, which mainly treats domestic wastewater (60%–70%) and brewery wastewater (30%–40%). The initial mixed liquor suspended solid (MLSS) in the SBR was 3,100 mg/L. The inoculated sludge was domesticated for 20 d, and then divided between the four SBR. The C/N ratio was calculated as the ratio of chemical oxygen demand (COD) to total nitrogen (TN) measured in mg/L, and the C/N ratio in the four reactors was 0, 5, 10, and 15, respectively. The reactors were then referred to as R_0, R_5, R_{10}, and R_{15}. R_{15} represented a carbon-excess case; R_5 and R_{10} both represented the condition of conventional activated sludge treating municipal wastewater, while R_0 represented a carbon-limited case. The synthetic wastewater in R_5, R_{10}, and R_{15} contained 99.9% ethanol (300 mg/L) and in R_0 contained ethanol 0, NH_4Cl (20–60 mg/L), K_2HPO_4 (6 mg/L).

2.2. Analytical methods

2.2.1. Conventional analytical methods

NH_4^+–N, NO_3^-–N, NO_2^-–N, COD, MLSS, and MLVSS were examined according to the Standard Methods [21]. DO, pH, and temperature (*T*) were continuously monitored using a pH/oxi 3620 analyzer (WTW Company, Germany).

2.2.2. Extraction of EPS and determination of EPS components

The sludge was fully mixed prior to commencing the extraction procedure. Slurry-water mixture at 4°C was centrifuged at 2,100×g for 10 min to separate solids from the supernatant. The supernatant was then filtered through a 0.45 μm microporous membrane, and the collected supernatant was regarded as the LB-EPS of the sludge sample. The residual sludge was resuspended in a Ringer solution, and the mixture was heated at 80°C for 60 min. Finally, the mixture at 4°C was centrifuged at a force of 12,000×g for 10 min to separate the solids from the supernatant, and the supernatant was then filtered through a 0.45 μm microporous

Table 1
Excitation and emitting (ex/em) wavelengths of fluorescence region

Region	Substance	ex/em wavelengths (nm)
I	Tyrosine-like protein	200–250/280–330
II	Tryptophan-like protein	200–250/330–380
III	Fulvic acid-like organics	200–250/380–500
IV	Soluble microbial by-product	250–400/280–380
V	Humic acid-like organics	250–400/380–500

membrane. The collected supernatant was subsequently regarded as the TB-EPS of the sludge sample. The sum of LB-EPS and TB-EPS thus represented the total EPS, and the quantity of polymers extracted was related to the SS content of the sludge.

PN was determined using the Coomassie brilliant blue method, and bovine serum albumin was used as the standard material. PS was determined using the phenol–sulfuric acid method, and glucose was used as the standard material. Furthermore, NA was determined using the ultraviolet absorption method [22].

2.2.3. 3D-EEM fluorescence spectroscopy and FRI analysis

The extracted EPS filtrate was measured by EEM fluorescence spectroscopy in a 1 cm quartz cuvette using an FP-6500 spectrofluorometer (Tokyo, Japan) at 25°C. Each EEM plot was generated by scanning excitation wavelengths from 220 to 400 nm at 5 nm steps and emitting fluorescence between 250 and 500 nm at 1 nm steps, with a scanning speed of 2,000 nm/min. To partially account for Rayleigh scattering, the fluorometer's response to a blank solution was subtracted from the fluorescence spectra recorded for samples [23]. Raman scattering was regulated using interpolation [24].

The FRI technique was adopted for EEM spectral data analysis [23,25]. EEM peaks were divided into five regions (Table 1). The FRI technique was developed to integrate the area beneath the EEM spectra. The volume beneath Region I of the EEM was Φ_i, and the normalized ex/em area volumes ($\Phi_{i,n}$, $\Phi_{T,n}$) were calculated using Eqs. (1) and (2):

$$\Phi_{i,n} = MF_i\Phi_i = MF_i\sum_{ex}\sum_{em}I\left(\lambda_{ex}\lambda_{em}\right)\Delta\lambda_{ex}\Delta\lambda_{em} \qquad (1)$$

$$\Phi_{T,n} = \sum\Phi_{i,n} \qquad (2)$$

where λ_{ex} is the excitation wavelength interval (taken as 5 nm), λ_{em} is the emission wavelength interval (taken as 1 nm), and $I(\lambda_{ex}\lambda_{em})$ is the fluorescence intensity (au) at each excitation–emission wavelength pair. Furthermore, MF_i is the multiplication factor, which is equal to the inverse of the fractional projected excitation–emission area.

The percentage fluorescence response ($P_{i,n}$, %) was calculated using Eq. (3) as follows:

$$P_{i,n} = \frac{\Phi_{i,n}}{\Phi_{T,n}}\times100\% \qquad (3)$$

3. Results and discussion

3.1. Effect of C/N ratio on EPS, TB-EPS, and LB-EPS

A comparison among the EPS, TB-EPS, and LB-EPS contents of the different reactors (with different C/N ratios) is shown in Fig. 1. The LB-EPS contents of all sludge samples were low (2–5 mg/g SS), but the TB-EPS contents showed to be much higher (14–46 mg/g SS). The contents of EPS and TB-EPS all increased remarkably from 18 and 14 to 40.7 and 37.5, when the C/N ratio increased from 0 to 5, and increased slightly from 42.9 and 40.3 to 48.9 and 45.8,

when the C/N ratio increased from 10 to 15, which indicates that the C/N ratio was positively correlated with the EPS and TB-EPS contents (Fig. 1b). Owing to the dominant component of TB-EPS in the total EPS and its changed under different C/N ratios, the sum of EPS changed remarkably. The findings were consistent with the results of the previous studies [10]. In addition, the C/N ratio had no significant impact on LB-EPS in this study (Fig. 1b), although other researchers have found that the C/N ratio has a significant effect on LB-EPS and its components. Such as, Wang et al. [9] determined that the PN content and the PN/PS ratio in LB-EPS increased with a decrease in the C/N ratio, whereas the PS content in LB-EPS decreased, and Ye et al. [8] found that the PS content in LB-EPS increased but the PN content decreased when the C/N ratio increased. In this study, due to low content of LB-EPS (Fig. 1c), LB-EPS change slightly under different C/N ratios (Fig. 1b). Therefore, further investigations of effect of C/N ratio on constituents and structural characteristics of LB-EPS using 3D-EEM in the following sections.

3.2. Effect of C/N ratio on EPS, TB-EPS, and LB-EPS components

The effect of the C/N ratio on PN, PS, and NA in EPS, TB-EPS, and LB-EPS can be seen in Fig. 2 and Table 2. There was an upward trend in the PN, PS, and NA contents of EPS and TB-EPS with an increase in the C/N ratio (Figs. 2a and b, Table 2). When the C/N ratio increased from 0 to 5, from 5 to 10 and from 10 to 15, the polysaccharide, protein, and nucleic acid contents in TB-EPS, respectively,
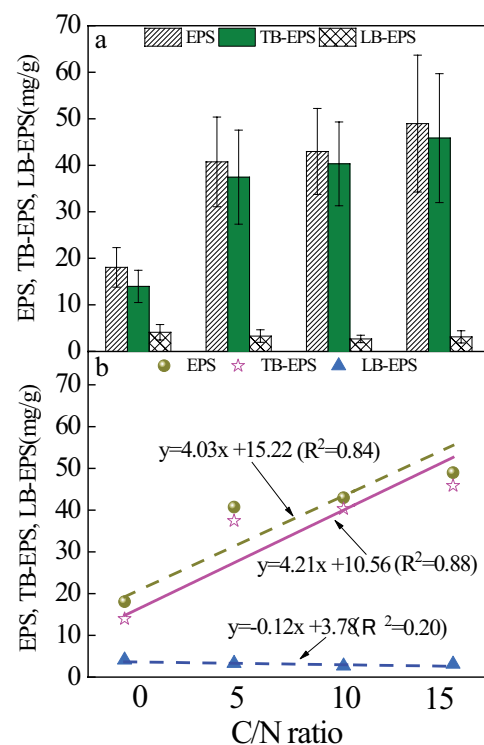
Fig. 1. (a) Effect of C/N ratio of the effluent on the total amount of EPS, TB-EPS and LB-EPS and (b) correlation between C/N ratio and contents of EPS, TB-EPS and LB-EPS.
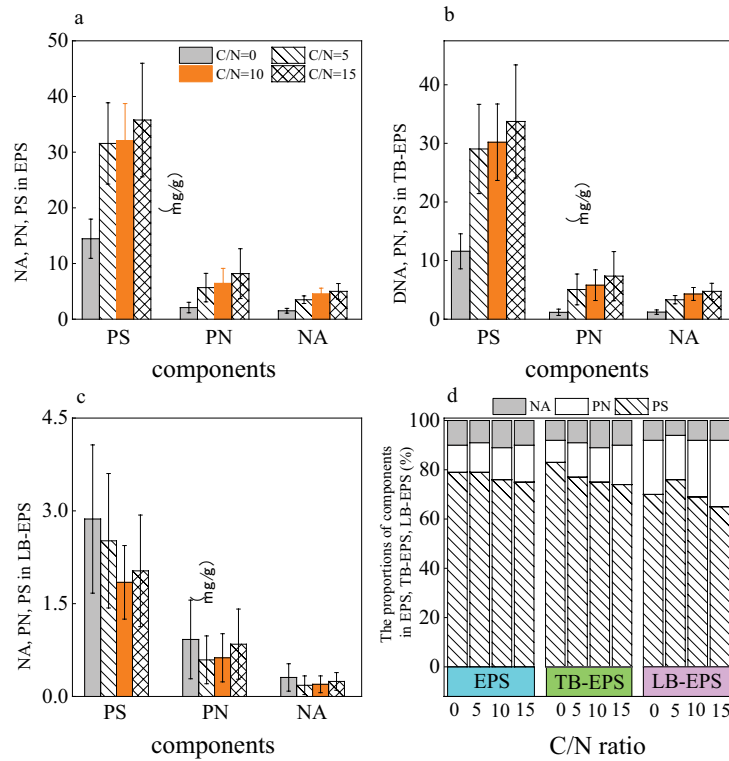
Fig. 2. (a) Effect of C/N ratio of the effluent on PN, PS and NA in EPS, (b) effect of C/N ratio of the effluent on PN, PS and NA in TB-EPS, (c) effect of C/N ratio of the effluent on PN, PS and NA in LB-EPS, and (d) the proportions of components in EPS, TB-EPS, LB-EPS under different C/N ratio.

Table 2
Components of EPS and their proportions in EPS (mg/gSS)

Systems	Components in EPS			Components in TB-EPS			Components in LB-EPS			Proportion of components in EPS (%)			Proportion of components in TB-EPS (%)			Proportion of components in LB-EPS (%)		
	PS	PN	NA	PS	PN	NA	PS	PN	NA	PS	PN	NA	PS	PN	NA	PS	PN	NA
R_0	14.4	2.1	1.5	11.6	1.2	1.2	2.9	0.92	0.31	79	11	10	83	9	8	70	22	8
R_5	31.5	5.7	3.5	29.1	5.1	3.3	2.5	0.59	0.18	79	12	9	77	14	9	76	18	6
R_{10}	32.0	6.4	4.5	30.2	5.8	4.3	1.8	0.63	0.20	76	13	11	77	14	11	69	23	8
R_{15}	35.7	8.2	5.0	33.7	7.3	4.8	2.0	0.85	0.24	75	15	10	74	16	10	65	27	8

increased by approximately 150%, 4%, and 11%; 325%, 14%, and 26% and 175%, 30%, and 11%, resulting in increased content of EPS. These results show that the C/N ratio has a significant effect on the components in EPS and TB-EPS and that the C/N ratio is positively correlated with their PN, PS, and NA contents. The influence of the C/N ratio on PS in TB-EPS was particularly obvious, similar results have been reported in other studies [10]. On the other hand, as the C/N ratio increased from 0 to 5, the change extent of PS, PN, and NA contents was obviously higher than the variations of components in TB-EPS when the C/N ratio increased from 5 to 15. It clearly appears that carbon source was the dominant member of the change of EPS under different C/N ratio, at the high C/N ratio, microorganisms can utilize the excess

carbon in the synthesis of cells and also in PS production [22,26]. Meanwhile, the nitrogen was used in the synthesis of proteins and nucleic acid by microorganisms and the synthesis of protein and nucleic acids requires energy, thus the high C/N ratio promoted the metabolization of PN and NA by microorganisms. Simultaneously, Chen et al. [27] reported that the PN content was affected by nitrogen (NH_4Cl) and the PN content was inversely proportional to nitrogen content in activated sludge. In addition, the components of LB-EPS in the C/N ratio of 0, respectively, were (116, 161, and 145, PS)%, (156, 146, and 108, PN)% and (172, 155, and 129, NA)% higher than the C/N ratio of 5, 10, and 15 (Fig. 2c, Table 2). The results showed that microorganisms living in bad surrounding (at the low C/N ratio, C/N = 0)

secreted more polysaccharide, protein, and nucleic acid contents on the outer layer of sludge floc, besides, the polysaccharide slightly increased and the protein and nucleic acid contents decreased when the C/N ratio increased from 5 to 15, resulting in slightly changed content of LB-EPS as the C/N ratio increased from 5 to 15. However, some researchers believed that the C/N ratio had no effect on the contents of PN and PS in EPS and TB-EPS, but an obvious effect on the contents of PN and PS in LB-EPS. Ye et al. [8] and Wang et al. [9] considered that the C/N ratio was negatively correlated with the PN and PS contents in LB-EPS.

As shown in Fig. 2d and Table 2, under the four C/N ratios, PS, PN, and NA, respectively, accounted for 65%~83%, 9%~27%, and 8%~11% of EPS, TB-EPS, and LB-EPS. Therefore, PS was the dominant component in EPS, TB-EPS, and LB-EPS, followed by PN, and the NA was least, similar results were reported in other studies [8,28]. Nevertheless, some researchers [29–31] found that the PN was the dominant component in EPS, besides Ton-That et al. [31] stated that the PN was the principal component in EPS and the production of PN was not hugely affected by the type of substrates used for microbial growth.
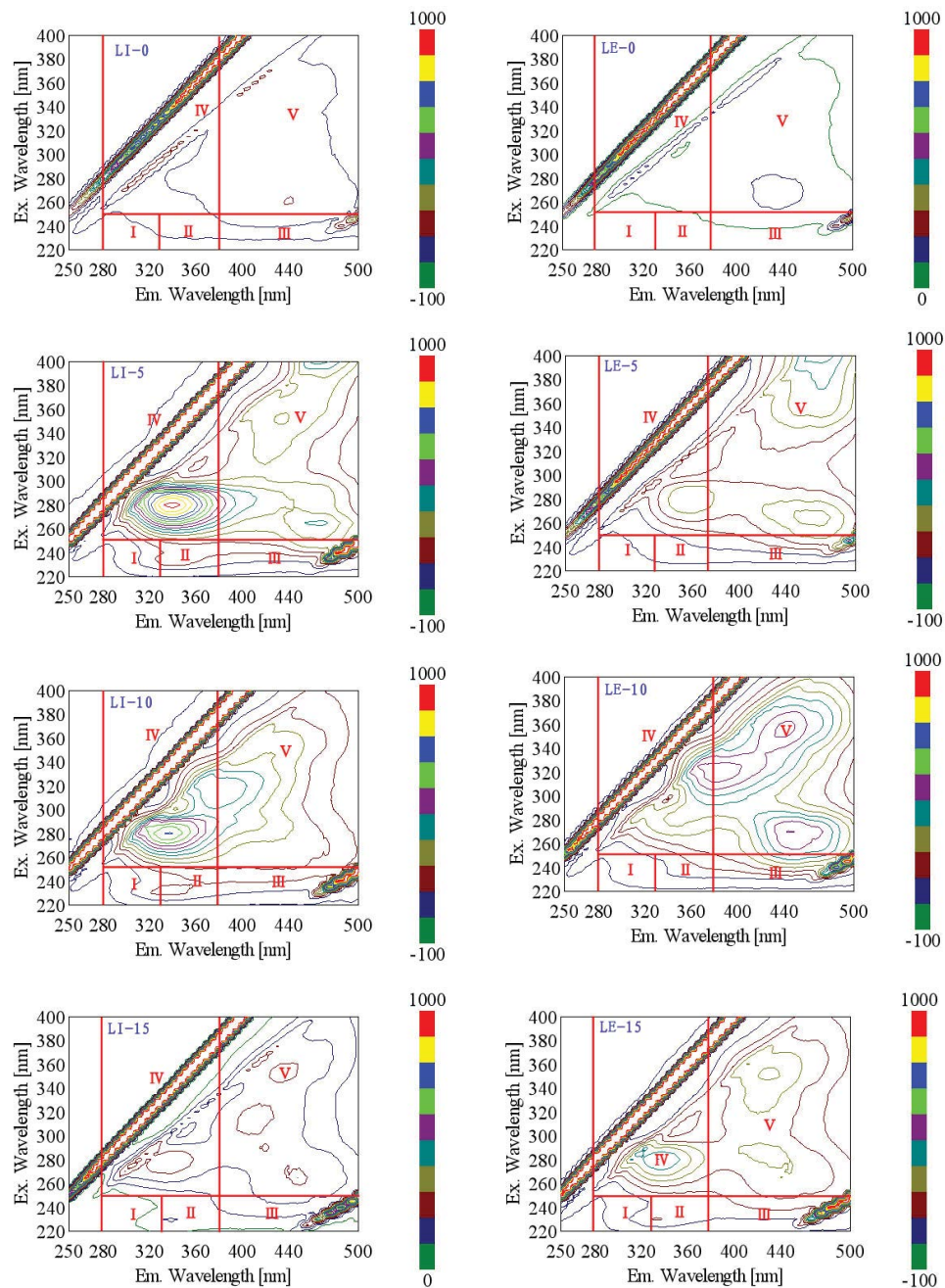

Fig. 3. EEM spectra of LB-EPS (LI-0, LI-5, LI-10, and LI-15: the influent LB-EPS of the C/N ratio of 0, 5, 10, and 15; LE-0, LE-5, LE-10, and LE-15: LB-EPS of the C/N ratio of 0, 5, 10, and 15 after nitrification).

3.3. FRI analysis of LB-EPS and TB-EPS

3.3.1. FRI technique assessment of LB-EPS

The FRI technique was used in accordance with methods referred to in published literature [32,33] and the total and regional fluorescence intensities for each sample were calculated. The 3D-EEM fluorescence spectra of LB-EPS and TB-EPS are shown in Figs. 3 and 5, LB-EPS and TB-EPS could be used as carbon and energy source for microorganisms [2]; meanwhile, the protein-like substance tyrosine and tryptophan, fulvic acid–like and soluble microbial by-product substances in LB-EPS and TB-EPS could be biodegraded [17]. Therefore, in sedimentation period, the protein-like substance tyrosine and tryptophan, fulvic acid–like and soluble microbial by-product substances were biodegraded, resulting in no evident peaks of the influent LB-EPS and TB-EPS. To better understand the 3D-EEM fluorescence features of LB-EPS and TB-EPS, the FRI technique was used to quantitatively assess changes in the five ex/em regions (Figs. 4 and 6).

As shown in Figs. 4 and 6, the highest contributions of the percentage fluorescence response in the influent and effluent EPS (LB-EPS and TB-EPS) of the SBR in the four C/N ratio systems were 34%–63% and 30%–49% in Region V (humic acid–like organics) and Region IV (soluble microbial by-product), respectively, followed by the Region III (fulvic acid–like substances) of 5%–13%, the Region II (tryptophan-like) of 1%–4% and Region I (tyrosine-like) of 0.2%–1.6%, the findings were consistent with the results of the previous study [17]. However, Wei et al. [18] believed that Region IV (soluble microbial by-product-like) expressed the highest percentage in both LB-EPS and TB-EPS.

As shown in Figs. 3 and 4, the values of $P_{i,n}$ in the influent LB-EPS under the four C/N ratio systems, R_0, R_5, R_{10}, and R_{15}, were 0.75%, 0.94%, 1%, and 1.06%; 1.32%, 2.14%, 2.13%, and 2.17%; 6.21%, 6.36%, 6.72%, and 8.98%; 38.36%, 42.3%, 44.16%, and 37.4%; and 53.36%, 48.26%, 45.99%, and 50.39%, respectively, for Regions I, II, III, IV, and V, respectively.
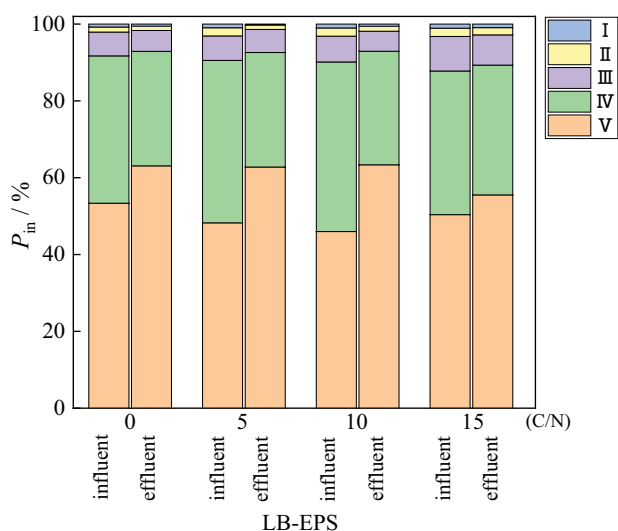

Fig. 4. Distribution of FRI in LB-EPS.

When the C/N ratio increased from 0 to 15, there were certain differences of $P_{i,n}$ in the influent LB-EPS, and the $P_{i,n}$ of Regions I and II (low fluorescence intensity) was not significantly different while that in Regions III, IV, and V was obviously different.

With an increase in the C/N ratio from 0 to 15, a significant increase in the fluorescence intensity was observed after nitrification. The normalized ex/em area volumes of Regions I, II, III, and IV in LB-EPS decreased after nitrification (Table 3), and the volume of Region V increased from 16,060; 41,080; 39,060; and 30,670 (au·nm²) to 20,340; 43,770; 60,470; and 36,320 (au·nm²) during nitrification. In addition, the changes (difference between effluent and influent in LB-EPS) of $P_{i,n}$ in R_0, R_5, R_{10}, and R_{15} were –0.2%, –0.71%, –0.42%, and –0.13%; –0.21%, –0.97%, –0.85%, and –0.3%; –0.7%, –0.36%, –1.51%, and –1.11%; and –8.57%, –12.5%, –14.6%, and –3.6%, respectively, presented in the Regions I, II, III, and IV. This result shows that the protein-like substance tyrosine and tryptophan, fulvic acid–like and soluble microbial by-product substances were biodegraded after nitrification, in particular, soluble microbial was high biodegradation rate (3%~14%). The changes of $P_{i,n}$ in Region V were 9.74%, 14.54%, 17.38%, and 5.14%, which implies that non-biodegraded humic acid was accumulated [34] and that this had a negative effect on further utilizing the waste sludge [17].

3.3.2. FRI technique assessment of TB-EPS

As shown in Figs. 5 and 6, the $P_{i,n}$ of the influent TB-EPS of the SBR in R_0, R_5, R_{10}, and R_{15} were 1.4%, 1.6%, 1.4%, and 1.6%; 3.6%, 3.9%, 3.9%, and 3.6%; 13.5%, 9.1%, 10.6%, and 11.8%; 42.3%, 44.5%, 42.2%, and 49%; and 39.2%, 40.9%, 41.9%, and 34%, respectively, presented in Regions I, II, III, IV, and V. When the C/N ratio increased from 0 to 15, the change in the $P_{i,n}$ of influent TB-EPS was similar to that of LB-EPS.

The normalized ex/em area volumes of Regions I, II, III, and IV in TB-EPS decreased after nitrification (Table 3), and the volume of Region V increased from 32,150; 30,820; 34,010; and 17,050 (au nm²) to 42,260; 32,910; 34,370; and 26,610 (au nm²)·during nitrification. And the changes (difference between effluent and influent in TB-EPS) of $P_{i,n}$ in R_0, R_5, R_{10}, and R_{15} were –0.3%, –0.2%, –0.2%, and –0.8%; –0.1%, –0.6%, –0.2%, and –0.8%; –3.4%, –1%, –0.9%, and –3.2%; and –8.3%, –5.1%, –3.1%, and –9.2%, respectively, presented in the Regions I, II, III, and IV. It was also suggested that the protein-like substance tyrosine and tryptophan, fulvic acid–like and soluble microbial by-product substances in TB-EPS were biodegraded after nitrification, especially soluble microbial was high biodegradation rate (3%~9%). The change of $P_{i,n}$ in Region V was (12.1, 6.9, 4.4, and 14)%, which suggests that humic acid was accumulated in TB-EPS at different C/N ratios.

Based on the above, the TB-EPS variations (difference between effluent and influent of TB-EPS) of $P_{i,n}$ of Regions I, II, III, IV, and V in R_0 (carbon-limited case) and R_{15} (carbon-excessed case) were higher than R_5 and R_{10} (the conditions of conventional activated sludge treating municipal wastewater); however, the LB-EPS variations (the difference value between effluent and influent of LB-EPS) of $P_{i,n}$ of Regions I, II, III, IV, and V in R_0 and R_{15} were lower than
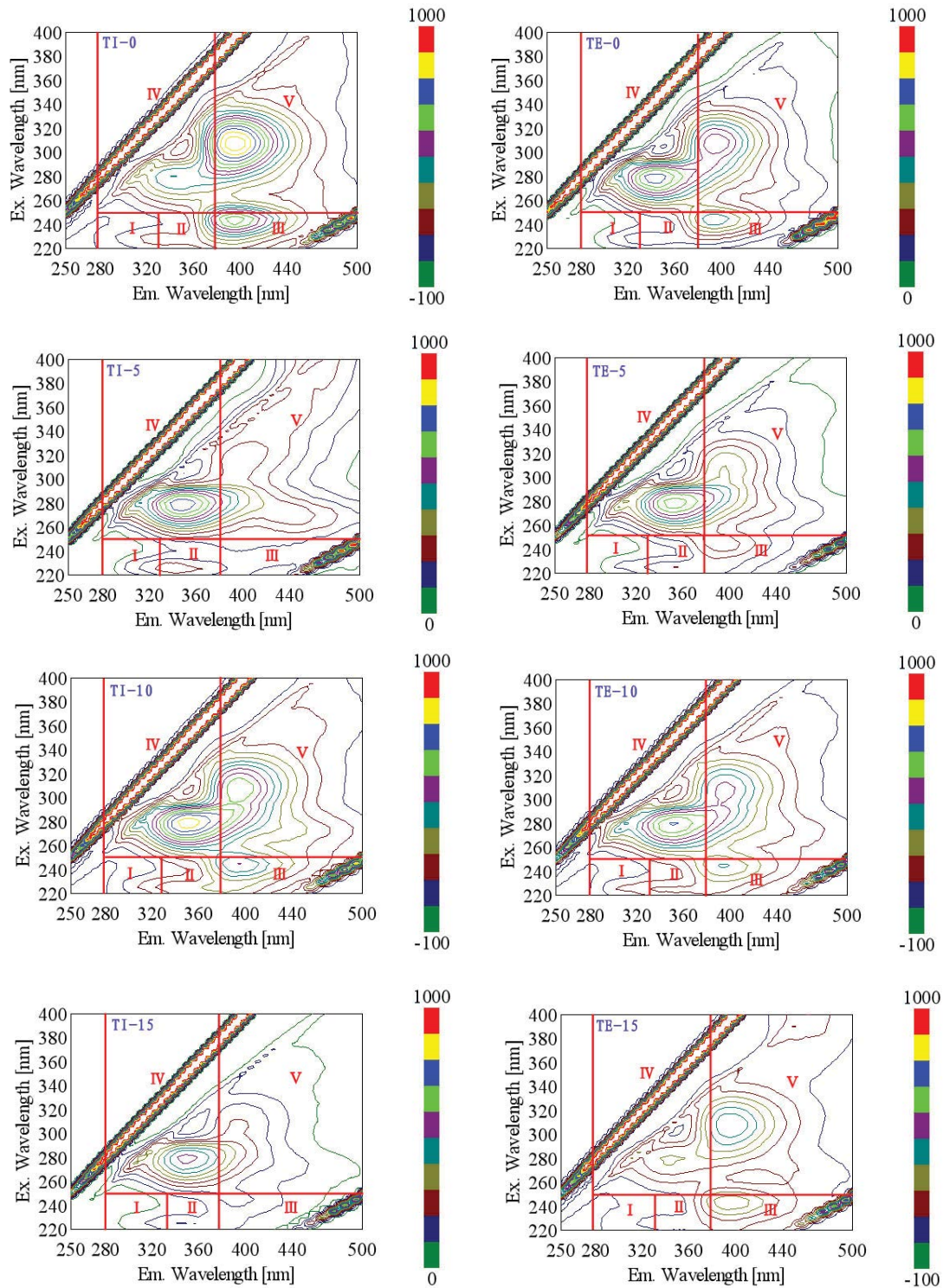
Fig. 5. EEM spectra of TB-EPS (TI-0, TI-5, TI-10, and TI-15: the influent TB-EPS of the C/N ratio of 0, 5, 10, and 15; TE-0, TE-5, TE-10, and TE-15: TB-EPS of the C/N ratio of 0, 5, 10, and 15 after nitrification).

R_5 and R_{10} (Figs. 3 and 4). It suggests that the major changes of the protein-like substance tyrosine and tryptophan, fulvic acid–like, soluble microbial and humic acid located in inner layer of sludge floc (TB-EPS) during nitrification at carbon-limited and carbon-excessed case, and the significant

changes of the organic compounds existed in outer layer of sludge floc (LB-EPS) under the conditions of conventional activated sludge treating municipal wastewater. Therefore, it is believed that diverse microbial species under different C/N ratio conditions cause variations in biodegradation and

Table 3
Normalized volume integral of different area in 3D-EEMs of EPS

| $\Phi_{i,n} \cdot 10^2$ (au·nm²)	Region	R_0		R_5		R_{10}		R_{15}	
		Influent	Effluent	Influent	Effluent	Influent	Effluent	Influent	Effluent
LB-EPS	I	2.3	1.8	8.0	1.6	8.5	5.5	6.5	6.1
	II	4.0	3.6	18.2	8.2	18.1	12.2	13.2	12.2
	III	18.7	17.6	54.1	41.8	57.1	49.7	54.7	51.5
	IV	115.5	96.0	360.1	207.7	375.1	282.1	227.6	221.1
	V	160.6	203.4	410.8	437.7	390.6	604.7	306.7	363.2
TB-EPS	I	11.5	9.1	12.1	9.6	11.4	8.9	8.0	4.4
	II	29.5	28.8	29.4	22.7	31.7	27.5	18.1	15.5
	III	110.7	83.2	68.6	55.8	86.0	72.0	59.2	47.7
	IV	346.9	280.1	335.3	271.3	342.5	290.3	245.7	220.6
	V	321.5	422.6	308.2	329.1	340.1	343.7	170.5	266.1
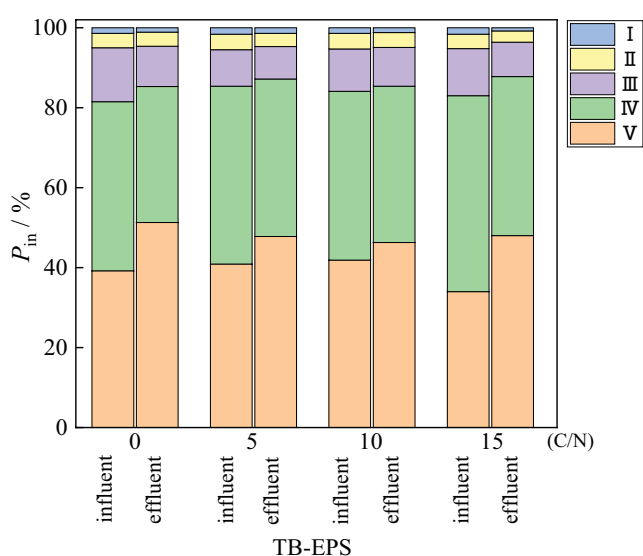
Fig. 6. Distribution of FRI in TB-EPS.

accumulation of microbial by-product substances during nitrification. However, it is necessary to analyze the detailed transformation of EPS during nitrification in SBRs.

In addition, the $P_{i,n}$ values of Regions I, II, III, IV, and V in TB-EPS, respectively, were 0.8%~1.6%, 2.8%~3.9%, 8%~13.5%, 34%~49%, and 34%~51%, and the $P_{i,n}$ values of Regions I, II, III, IV, and V in LB-EPS, respectively, were 0.23%~1.0%, 1.1%~2.1%, 5%~9%, 29%~44%, and 45%~63%. The percentage of protein-like substances tyrosine and tryptophan and fulvic acid–like and soluble microbial substances were dramatically higher in TB-EPS than in LB-EPS, but the $P_{i,n}$ value of humic acid in TB-EPS was considerably lower than that in LB-EPS.

4. Conclusions

This paper has presented a comparative study of influent and effluent EPS in SBR and its chemical constituents using 3D-EEM with FRI at different C/N ratio, the following conclusions may be drawn from this study as follows:

- With an increase in the C/N ratio from 0 to 15, there was an increase in the production of EPS, TB-EPS, and components in TB-EPS, but the PS, PN, and NA contents of LB-EPS at the C/N ratio of 0 were higher than those in other reactors of R_5, R_{10}, and R_{15}. Meanwhile, PS was the dominant component in EPS, TB-EPS, and LB-EPS under different C/N ratio.
- The highest $P_{i,n}$ of humic acid–like organics (34%~63%) and the $P_{i,n}$ of tyrosine-like (0.2%~1.6%) was the lowest in both types of EPS fractions.
- The protein-like substance tyrosine and tryptophan, fulvic acid–like, and soluble microbial by-product substances were biodegraded and non-biodegraded humic acid was accumulated in TB-EPS and LB-EPS after nitrification.
- The $P_{i,n}$ value of humic acid in TB-EPS was dramatically lower than that in LB-EPS.

Author contributions

C.Z. Chen, and K.Q. Du: Conceptualization, Methodology, Software; C.Z. Chen and S.B. Liu: Data curation, Writing-Original draft preparation; K.Q. Du, Z. Wei and C.Z. Chen: Visualization, Investigation; H.W. Sun and H.G. Liu: Supervision; J.F. Li and Q.G. Wang: Software, Validation; J.F. Li, H.W. Sun and Y.C. Ren: Writing-Reviewing and Editing; J.F. Li: project administration and funding acquisition.

References

[1] X.Y. Li, S.F. Yang, Influence of loosely bound extracellular polymeric substances (EPS) on the flocculation, sedimentation and dewaterability of activated sludge, Water Res., 41 (2007) 1022–1030.

[2] G.P. Sheng, H.Q. Yu, X.Y. Li, Extracellular polymeric substances (EPS) of microbial aggregates in biological wastewater treatment systems: a review, Biotechnol. Adv., 28 (2010) 882–894.

[3] G.P. Sheng, H.Q. Yu, Characterization of extracellular polymeric substances of aerobic and anaerobic sludge using three-dimensional excitation and emission matrix fluorescence spectroscopy, Water Res., 40 (2006) 1233–1239.

[4] Y.H. Shi, J.H. Huang, G.M. Zeng, Y.L. Gu, Y.N. Chen, Y. Hu, B. Tang, J.X. Zhou, Y. Yang, L.X. Shi, Exploiting extracellular polymeric substances (EPS) controlling strategies for performance enhancement of biological wastewater treatments: an overview, Chemosphere, 180 (2017) 396–411.

[5] H. Liu, H.H.P. Fang, Extraction of extracellular polymeric substances (EPS) of sludges, J. Biotechnol., 95 (2002) 249–256.

[6] X.Y. Fan, Y.L. Wang, D.X. Zhang, Y.J. Guo, S.H. Gao, E.R. Li, H.L. Zheng, Effects of acid, acid-ZVI/PMS, Fe(II)/PMS and ZVI/PMS conditioning on the wastewater activated sludge (WAS) dewaterability and extracellular polymeric substances (EPS), J. Environ. Sci., 91 (2020) 73–84.

[7] X.L. Huangfu, Y.H. Xu, C.H. Liu, Q. He, J. M, C.H. Ma, R.X. Huang, A review on the interactions between engineered nanoparticles with extracellular and intracellular polymeric substances from wastewater treatment aggregates, Chemosphere, 219 (2019) 766–783.

[8] F.X. Ye, Y.F. Ye, Y. Li, Effect of C/N ratio on extracellular polymeric substances (EPS) and physicochemical properties of activated sludge flocs, J. Hazard. Mater., 188 (2011) 37–43.

[9] Z. Wang, M. Gao, Y. Xin, D. M, Z.L. She, Z.Wang, C.Q. Sun, Y. Ren, Effect of C/N ratio on extracellular polymeric substances of activated sludge from an anoxic-aerobic sequencing batch reactor treating saline wastewater, Environ. Technol., 35 (2014) 2821–2828.

[10] A.P. Miqueleto, C.C. Dolosic, E. Pozzi, E. Foresti, M. Zaiat, Influence of carbon sources and C/N ratio on EPS production in anaerobic sequencing batch biofilm reactors for wastewater treatment, Bioresour. Technol., 101 (2010) 1324–1330.

[11] R.K. Henderson, A. Baker, K.R. Murphy, A. Hambly, R.M. Stuetz, S.J. Khan, Fluorescence as a potential monitoring tool for recycled water systems: a review, Water Res., 43 (2009) 863–881.

[12] L.Y. Yang, J. Hur, W.N. Zhuang, Occurrence and behaviors of fluorescence EEM-PARAFAC components in drinking water and wastewater treatment systems and their applications: a review, Environ. Sci. Pollut. Res., 22 (2015) 6500–6510.

[13] F.C. Marhuenda-Egea, E. Martinez-Sabater, J. Jorda, R. Moral, M.A. Bustamante, C. Paredes, M.D. Pérez-Murcia, Dissolved organic matter fractions formed during composting of winery and distillery residues: evaluation of the process by fluorescence excitation–emission matrix, Chemosphere, 68 (2007) 301–309.

[14] W. Tian, L.Z. Li, F. Liu, Z.H. Zhang, G.H. Yu, Q.R. Shen, B. Shen, Assessment of the maturity and biological parameters of compost produced from dairy manure and rice chaff by excitation–emission matrix fluorescence spectroscopy, Bioresour. Technol., 110 (2012) 330–337.

[15] G.Y. Zhen, X.Q. Lu, B.Y. Wang, Y.C. Zhao, X.L. Chai, D.J. Niu, A.H. Zhao, Y.Y. Li, Y. Song, X.Y. Cao, Synergetic pretreatment of waste activated sludge by Fe(II)-activated persulfate oxidation under mild temperature for enhanced dewaterability, Bioresour. Technol., 124 (2012) 29–36.

[16] X. Jia, C.W. Zhu, M.X. Li, B.D. Xi, L.J. Wang, X. Yang, X.F. Xia, J. Su, A comparison of treatment techniques to enhance fermentative hydrogen production from piggery anaerobic digested residues, Int. J. Hydrogen Energy, 38 (2013) 8691–8698.

[17] L. Guo, M.M. Lu, Q.Q. Li, J.W. Zhang, Y. Zong, Z.L. She, Three-dimensional fluorescence excitation–emission matrix (EEM) spectroscopy with regional integration analysis for assessing waste sludge hydrolysis treated with multi-enzyme and thermophilic bacteria, Bioresour. Technol., 171 (2014) 22–28.

[18] D. Wei, T. Yan, K.Y. Zhang, Y. Chen, N. Wu, B. Du, Q. Wei, Qualitative and quantitative analysis of extracellular polymeric substances in partial nitrification and full nitrification reactors, Bioresour. Technol., 240 (2017) 171–176.

[19] J. Sun, L. Guo, Q.Q. Li, Y.G. Zhao, M.C. Gao, Z.L. She, C.J. Jin, Three-dimensional fluorescence excitation–emission matrix (EEM) spectroscopy with regional integration analysis for assessing waste sludge hydrolysis at different pretreated temperatures, Environ. Sci. Pollut. Res., 23 (2016) 24061–24067.

[20] F.X. Ye, G. Peng, Y. Li, Influences of influent carbon source on extracellular polymeric substances (EPS) and physicochemical properties of activated sludge, Chemosphere, 84 (2011) 1250–1255.

[21] A.D. Eaton, L.S. Clesceri, A.E. Greenberg, M.A.H. Franson, Standard Methods for the Examination of Water and Wastewater, Am. J. Public Health Nations Health, 56 (1995) 387–388.

[22] Y. Mengistu, C. Edwards, J.R. Saunders, Continuous culture studies on the synthesis of capsular polysaccharide by *Klebsiella pneumoniae* K1, J. Appl. Bacteriol., 76 (1994) 424–30.

[23] W. Chen, P. Westerhoff, J.A. Leenheer, K. Booksh, Fluorescence excitation–emission matrix regional integration to quantify spectra for dissolved organic matter, Environ. Sci. Technol., 37 (2003) 5701–5710.

[24] G.H. Yu, M.J. Wu, Y.H. Luo, X.M. Yang, W. Ran, Q.R. Shen, Fluorescence excitation–emission spectroscopy with regional integration analysis for assessment of compost maturity, Waste Manage., 31 (2011) 1729–1736.

[25] Y.D. Guo, L. Guo, M. Sun, Y.G. Zhao, M.C. Gao, Z.L. She, Effects of hydraulic retention time (HRT) on denitrification using waste activated sludge thermal hydrolysis liquid and acidogenic liquid as carbon sources, Bioresour. Technol., 224 (2017) 147–156.

[26] Z.M. Zhang, R.J. Cao, L.N. Jin, W.T. Zhu, Y.T. Ji, X.Y. Xu, L. Zhu, The regulation of N-acyl-homoserine lactones (AHLs)-based quorum sensing on EPS secretion via ATP synthetic for the stability of aerobic granular sludge, Sci. Total Environ., 673 (2019) 83–91.

[27] Y.Y. Chen, S.P. Ju, D.J. Lee, Aerobic granulation of protein-rich granules from nitrogen-lean wastewaters, Bioresour. Technol., 218 (2016) 469–475.

[28] S.F. Yang, X.Y. Li, Influences of extracellular polymeric substances (EPS) on the characteristics of activated sludge under non-steady-state conditions, Process Biochem., 44 (2009) 91–96.

[29] B. Frølund, R. Palmgren, K. Keiding, P.H. Nielsen, Extraction of extracellular polymers from activated sludge using a cation exchange resin, Water Res., 30 (1996) 1749–1758.

[30] Y. Liu, C.H. Yang, J. Li, Influence of extracellular polymeric substances on *Pseudomonas aeruginosa* transport and deposition profiles in porous media, Environ. Sci. Technol., 41 (2007) 198–205.

[31] H. Ton-That, L.A. Marraffini, O. Schneewind, Protein sorting to the cell wall envelope of Gram-positive bacteria, Biochim. Biophys. Acta-Mol. Cell Res., 1694 (2004) 269–278.

[32] T. Anumol, M. Sgroi, M. Park, P. Roccaro, S.A. Snyder, Predicting trace organic compound breakthrough in granular activated carbon using fluorescence and UV absorbance as surrogates, Water Res., 76 (2015) 76–87.

[33] M. Sgroi, P. Roccaro, G. Oelker, S.A. Snyder, N-nitroso-dimethylamine (NDMA) formation during ozonation of wastewater and water treatment polymers, Chemosphere, 144 (2016) 1618–1623.

[34] J. Jimenez, E. Gonidec, J.A.C. Rivero, E. Latrille, F. Vedrenne, J.P. Steyer, Prediction of anaerobic biodegradability and bioaccessibility of municipal sludge by coupling sequential extractions with fluorescence spectroscopy: towards ADM1 variables characterization, Water Res., 50 (2014) 359–372.